New Solutions of the Electronic Circuits of High Speed Optical Receivers.

Summary of Ph.D. thesis

Attila Zólomy

Supervisors:

Dr. András Baranyi

Dr. Tibor Berceli

August, 2003
Budapest

Introduction

The highest growing sectors of the economy in the last two decades are the informatics and telecommunication. Their development is very correlated, due to the fact that the fast and efficient process of information requires transportation of it with extremly high speed as well. The new technical possibilities led to new applications, which are the base of novel industry sectors. They are essential for economical prosperity (high-speed computer networks, Internet). Recently, the Internet became the main information source of professional users in many areas (technical and natural science, research, development, commerce etc.), and on the other hand it is a strong fortress of democracy.

One of the main properties of these kind of applications, that due to the demand for higher speed and better quality, they require higher and higher data rate. It can be fullfilled only by fiber optic networks due to the low capacity of coaxial lines and long haul radio links. Beside that, the latter suffers from the lack of free radio channels, bandwidth restrictions and interference or propagation problems. According to this, huge efforts are made to further improve the building parts and circuits of the optical networks.

One of the main restriction factors is the bandwidth of the electronic parts and of the E/O and O/E converters of these systems, as the optical fibers have several order higher capacity. Hence, research and development of amplifiers, multiplexers, demultiplexers, optical modulators, photodiodes with extremly high bandwidth became very important.

Great efforts are invented to the research of optically feeded mobile radio systems (so called radio over fiber systems). The mobile communication is one of the fastes growing field of telecommunication. Due to the enormous increasing of the user number and the absence of free radio channels, the following tendencies can be observed in the future:

- Increasing cell number with decreasing size (picocell systems)
- Higher cell capacity
- Usage of MMW or higher frequency ranges.

According to that, the base stations will be feeded through optical networks, and the MMW carrier will be generated by optical methods or electricaly from an optically transmitted subharmonic reference.

The thesis deals with electronic circuits mainly applied in high speed optical receivers, but the quite general results are well applicable in the design of the transmitter's electronics as well.
The thesis consists of two main parts.

- The first five chapters is devoted to the analysis and synthesis of ultra wideband distributed amplifiers usually applied in high speed optical receivers. The goal is to achieve flat gain characteristics with maximum gain-bandwidth product. Noise and nonlinear analysis is not included due to it's comprehensive discussion in the literature and size constrains.
- In the 6^{th} chapter new method is presented for the analysis and synthesis of harmonic oscillators. This circuit is applied in a new picocell system proposed by Prof. Tibor Berceli, in which the MMW carrier is generated from an optically transmitted subcarrier as a reference.

The first main part comprises five chapters:

The first chapter is a comprehensive review of the distributed amplifier's analysis and synthesis methods available in the literature.

The second chapter deals with lumped element distributed amplifiers, in which lumped inductances interconnects the transistors. The effect of the parasitic connection inductances of the active devices, the phase mismatch between the input and output artificial transmission lines of the amplifier and the input and output reflections are also discussed. Conclusions are well applicable in the more complicated cases of the following chapters.

The third chapter analyses the so-called distributed element amplifiers in which transmission lines replace the lumped inductances between the transistors.

The first part of the fourth chapter compares the gain bandwidth product of the distributed element amplifier to that of the lumped element one. It proves that the lumped element amplifier has the highest gain-bandwidth product, thus the reduction of the transmission line size is important. The section also gives formulas to the applied transmission line impedance to maintain the image impedances of the amplifier's lines on a desired value independently of the transmission line length. By this way, the phase shift per section of the amplifier's input or output line, and thus the phase mismatch between them can be varied independently of the termination impedances.

Based on the previous results the second part of the fourth chapter gives a new design method. It yields a distributed element amplifier with the highest gain-bandwidth product with flat gain in the

presence of the parasitic connection inductances, by the proper adjust of the phase mismatch between the amplifier's input and output lines.

The fifth chapter shows several realized distributed amplifiers.

The second main part of the thesis consists of the sixth chapter.

Subsection 6.1 describes a millimeter wave carrier generation method, which uses an optically transmitted subharmonic signal as a reference. The frequency multiplication is optained by a PLL applying harmonic VCO. These system was realized on the framework of the FRANS research project of the E.U.

The further subsections are deals with the details of the analysis and design of VCO's with high third harmonic content. A theoretical analysis is presented based on the method developed by Bíró [60]. Using the results a design method is presented for MESFET harmonic oscillators. The predicted fundamental and 3rd harmonic output power levels are compared to that of a realized oscillator.

Distributed amplifier

The distributed amplifier has the highest bandwidth (several decades) among the known amplifier structures. Due to this and the low noise level (F=2-5 dB) it is ideal as a front-end amplifier in optical receivers.

Percival first proposed the DA structure in 1936. In his patent he connected the capacitive input and output pins of several active devices by lumped inductances. The resulted input and output low pass artificial transmission lines incorporated the active device capacitances and by this way the gain-bandwidth product (GBP) exceeded the GBP of simple parallel connected active devices.

The general schematic of an N stage distributed amplifier is shown in Fig. 1. The input and output DA lines are formed by the active devices input and output admittance and by the interstage inductances or at higher frequencies by transmission lines. The DA lines are terminated by their image impedances (denoted by Z_{GL} and Z_{DL}). It can be either the T (mid series) or Π (mid shunt) image impedance (denoted by Z_{0T} and $Z_{0\Pi}$) depending the end structure of the amplifier (T- or Π-section). In loss free case the image impedances are pure real below the cut-off frequency of the line and pure imaginary above that. The Z_{0T} impedance is monotonically decreases, the $Z_{0\Pi}$ impedance monotonically increases below cut off. The former has a zero the latter has a pole at cut off.

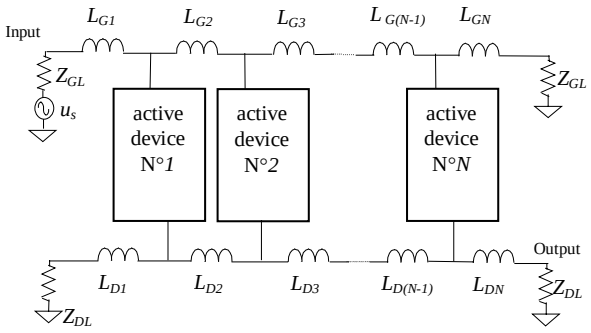

Fig. 1. Schematic of DA

The input signal propagates from the generator to the right hand side termination of the input line and drives the active device inputs. The signals coming from the active devices are added in phase by the output line toward the output. By this way the voltage gain and the power gain is proportional to N and N^2, respectively. In loss free case the propagation factor (denoted by θ) is pure imaginary and linear with frequency below and pure real above cut-off. Hence above their cut-off the DA lines have a strong attenuation and the amplifier is not operating.

THESIS GROUP 1.

The 1. thesis group deals with the analysis of the so called lumped element loss free distributed amplifiers, where lumped inductances interconnects the transistors.

The image impedances, propagation factor and the cut-off frequency can be calculated from the chain matrix of a T-section or a Π-section of the DA lines using network theory methods. The voltage or current gain of the k^{th} signal route in the amplifier can be calculated by multiplying the voltage or current gains of the T-sections in it and the gain of the so-called transfer T-section which incorporates the k^{th} active device, and has an input at the input line and an output at the output line. The gain of the whole amplifier is the sum of the gains of the indicidual routes. The power gain can be calculated from the voltage and current gain.

In the very ideal case the active devices is comprises only the input and output capacitances and the transconductance. In this case the DA lines have LC ladder low pass structure. The image impedances are proportional to the square root of the L/C ratio, the cut-off frequency is inversely proportional to the square root of the LC product. For perfect matching the DA lines should be terminated by their frequency dependent image impedances (it is real below cut-off). However, due to realization difficulties the DA lines is usually terminated by constant impedances (typicaly by 50 Ohms). It causes mismatch at the upper side of the pass band. In case of a reflection restriction (f.e. $|\Gamma| \leq -20dB$), a so-called operation bandwidth can be defined in which the reflection is lower than the specified. The upper edge of the operation band (operation cut-off) is lower than the real cut-off. *The 1.1 thesis proposes new methods to increase the operation bandwidth (OB) and thus the operational gain-bandwidth product (OGBP) in case of constant termination impedances. The methods are briefly summarized in Table. 1.*

In case of T-section ending:	In case of Π-section ending :
1) decrease of termination impedance	3) increase of termination impedance
2) increase of Z_{0T} image impedance	4) decrease of $Z_{0\Pi}$ image impedance

Table 1.

The thesis als o gives formulas for the calculation of the necessary reduction or increase of the image or termination impedances to achieve the maximum increase of OB and predicts the variation of OGBP. The first case of Table 1 is demonstrated in Table 2 for several reflection specifications. The first row shows the operation cut-off normalized to the real cut-off (ω_{rel}) if the low frequency values of the image impedances are equal to the constant termination impedance (Z_L). The second row gives normalized OB if the termination impedance is properly reduced. The third row shows the reduction of the gain due to the mismatch, and the last row gives the predicted variation of the OGBP.

	$\omega_{\Gamma rel}\|_{\Gamma=-10dB}$	$\omega_{\Gamma rel}\|_{\Gamma=-16dB}$	$\omega_{\Gamma rel}\|_{\Gamma=-20dB}$
ω_{rel} if $Z_L=Z_0$	0.854	0.67	0.575
ω_{rel} if $Z_L = Z_0 \frac{1-\Gamma}{1+\Gamma}$	0.963	0.835	0.741
Gain reduction	0.9 dB	0.212 dB	0.086 dB
Variation of OGBP %	91.7	118	126

Table 2.

It is also shown that the phase mismatch between the input and output line of the DA can be adjusted by the second and fourth method of Table 1.

Thesis 1.1. It shows a general calculation method, which is well applicable for the calculation of the gain, image impedances, propagation factor of any DA structure applying unilateral active device model. It proposes the above mentioned method to reduce the refletion problems and increase the operational bandwidth in case of consatnt impedance termination of DA lines [S4, S5, S20, S11].

The gain normalized to its DC value, of an ideal, loss free, N stage DA is given by Eq. 1.

$$\Delta P(\omega_{rel}) = \frac{P(\omega_{rel})}{P(0)} = \frac{1}{N^2} \frac{1}{\left(\sqrt{1-\omega_{rel}^2 \frac{1}{q^2}}\right)^* \sqrt{1-\omega_{rel}^2}} \left| \frac{\sin(\frac{N}{2}\Delta\theta)}{\sin(\frac{\Delta\theta}{2})} \right|^2 \qquad 1$$

where q is the measure of the phase mismatch between the input (usually called gate) and output (usually called drain) line of the DA. It is the ratio of the input and output line cut-off frequency as it is given in Eq. 2.

$$q = \frac{Z_{0TG}(\omega=0)}{Z_{0TD}(\omega=0)} \frac{C_G}{C_D} = \frac{\omega_{CD}}{\omega_{CG}} = \frac{\sqrt{L_G C_G}}{\sqrt{L_D C_D}} \text{ ; as } \omega_C = \frac{2}{\sqrt{LC}} \qquad 2$$

In Eq. 1. the $\Delta\theta$ can be also given by the normalized operation frequency of the gate line and by q.

$$\Delta\theta = \theta_D - \theta_G = a\cosh(1-2\omega_{rel}^2 \frac{1}{q^2}) - a\cosh(1-2\omega_{rel}^2) \qquad 3$$

In case of phase sychrone ($\Delta\theta=\theta_D-\theta_G=0$, $q=1$) the gain of the DA has a pole at cut-off. By increasing q (introducing phase mismatch) at a given stage number the last part of Eq. 1 will have a monotonically decreasing gain characteristic with frequency. This phenomenon can decrease or compensate the effect of the pole at cut-off. The same behaviour can be observed if the stage number is increased in case of a fixed q. It is demonstarted in Fig. 2.a where Eq. 1 is shown vs. real frequency at different stage numbers ($q=2$, $C_G=0.4$ *pF*, $Z_0=50$ *Ohm*). As it can be observed, at a given q value only a definite stage number results flat gain. The higher the q value the lower the definite stage number and vica versa. The aim is to determine a stage number range which results a power gain deviation (normalized to its low frequency value) lower than a specified range (ΔP) at a given q value and normalized frequency (which is usually the operation cut-off determined by the termination impedance and refletion restriction). It can be done by solving Eq. 1 for N. However, it is a transcendental equation, thus can not be solved in closed form. By expanding the last part into taylor series an approximate solution can be achieved, which is given by Eq. 4. and is shown for several ΔP values in Fig. 2.b. for ideal, loss free case ($q=1.45$). As it can be observed the deviation is less than 1dB at $\omega_{rel}=0.8$ normalized frequency if $N=4$ or 5.

$$N(\omega_{rel},q,\Delta P)=\sqrt{\frac{40-\sqrt{-320+\left(1920-80\Delta\theta^2+\Delta\theta^4\right)\left(1-\omega_{rel}^2\right)^{1/4}\left(1-\frac{\omega_{rel}^2}{q^2}\right)^{1/4}\sqrt{\Delta P}}}{\Delta\theta^2}} \qquad 4$$

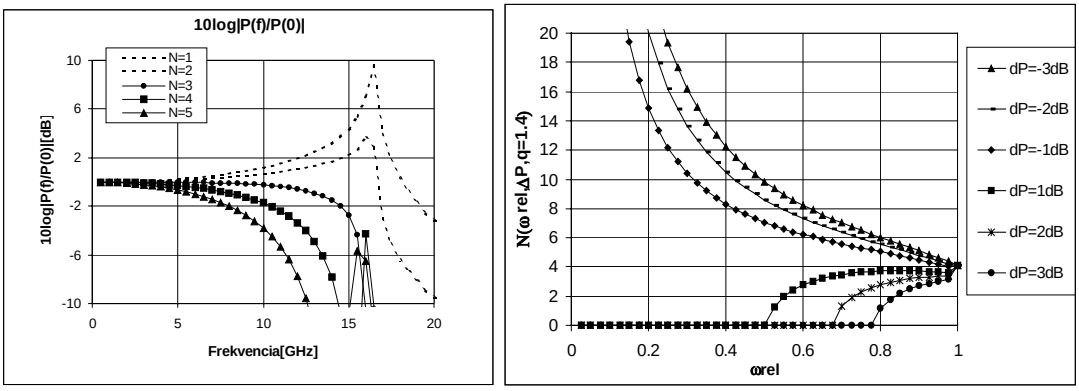

2.a) 2.b)

Very similar investigation is done for the presence of the parasitic connection inductances of the transistors.

Thesis 1.2. It investigates the effect of phase mismatch on the power gain characteristic. It gives approximate formulas for the proper stage number to achieve a specified gain deviation (ΔP) at a given frequency normalized to the input line cut-off and a given phase mismatch value (q). The same formulas are presented for the presence of the input and output parasitic connection inductances either by the conventional way i.e. they are series with the capacitances, or by the so called "V-shape connected" way, which will be detailed described in Thesis 1.3. The mentioned equation is also given for a hybrid structure in which the V-shape and the conventional connection method are applied at the transistors input and output, respectively [S2, S5, S7].

The schematic of a DA comprises the parasitic connection inductances in a conventional way is presented in Fig. 3.a. The power gain is given by Eq. 5. As it can be seen the presence of connection inductance (L_B) strongly reduces the cut-off frequency: it's effect for times stronger than that of the interstage inductance.

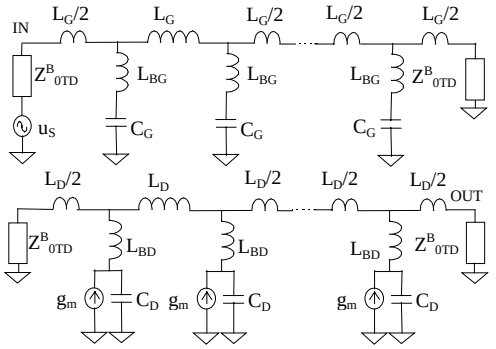

3.a)

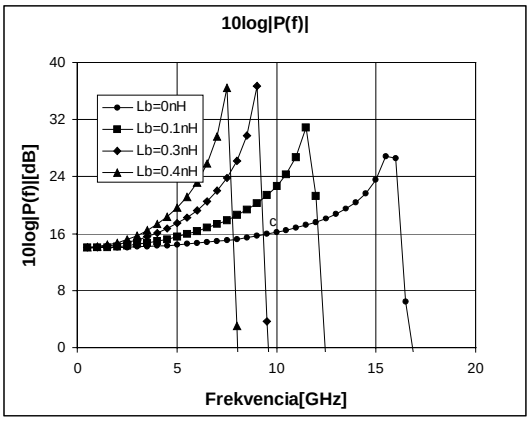

3.b)

It is also demonstarted in Fig. 3.b, where the power gain of a four stage DA is presented at different L_B values (*C=0.4 pF, Z0=50 Ohm*). This effect can be usefull if the aim is the effective tune of the phase mismatch by the reduction of the cut off of the actuall (usually output) line.

$$P^B = \frac{gm^2 \sqrt{\frac{L_G}{C_G}\frac{L_D}{C_D}}\, e^{-re\left(\theta_G^B-\theta_D^B\right)} e^{-2Nre(\theta_D^B)} \sum_{K=1}^{N} e^{K\left(\theta_D^B-\theta_G^B\right)} \sum_{K=1}^{N} e^{K\left(\theta_D^B-\theta_G^B\right)^*}}{4\left|1-\omega^2 C_D L_{BD}\right|\left|1-\omega^2 C_G L_{BG}\right|\sqrt{1-\omega^2 C_G\left(L_{BG}+\frac{L_G}{4}\right)}\left(\sqrt{1-\omega^2 C_D\left(L_{BD}+\frac{L_D}{4}\right)}\right)^*} \qquad 5$$

$$\omega_c^B = \frac{1}{\sqrt{C\left(L_B + L/4\right)}}$$

The harmfull effect of the connection inductances can be reduced if somehow they are transformed from the shunt arm to the series arm of the ladder structure of the line. This can be achieved by the so-called V-shape connection of the transistors. The schematic of a lumped element DA applying this structure is presented in Fig. 4.a. The power gain and the cut-off frequency is given by Eq. 6 and 7.

$$P^V = \frac{gm^2}{4} \frac{\sqrt{\frac{L_G+2L_{BG}}{C_G}}\sqrt{\frac{L_D+2L_{BD}}{C_D}}\, e^{re\left(\theta_G^V-\theta_D^V\right)} e^{-2N\, re\left(\theta_D^V\right)}}{\left(\sqrt{1-\omega^2\frac{\left(L_D+2L_{BD}\right)C_D}{4}}\right)^*\sqrt{1-\omega^2\frac{\left(L_G+2L_{BG}\right)C_G}{4}}} \sum_{K=1}^{N} e^{K\left(\theta_D^V-\theta_G^V\right)} \sum_{K=1}^{N} e^{K\left(\theta_D^V-\theta_G^V\right)^*} \qquad 6$$

$$\omega_c^V = \frac{2}{\sqrt{\left(L+2L_B\right)C}} \qquad 7$$

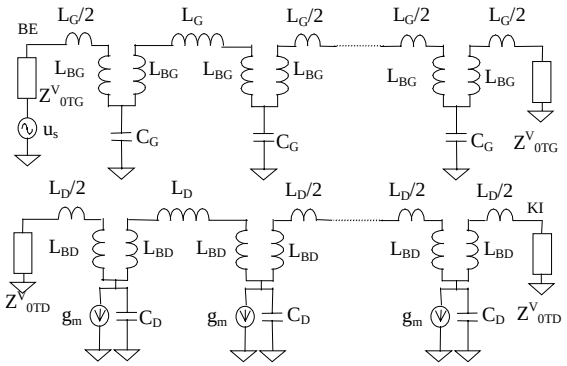

4.a)

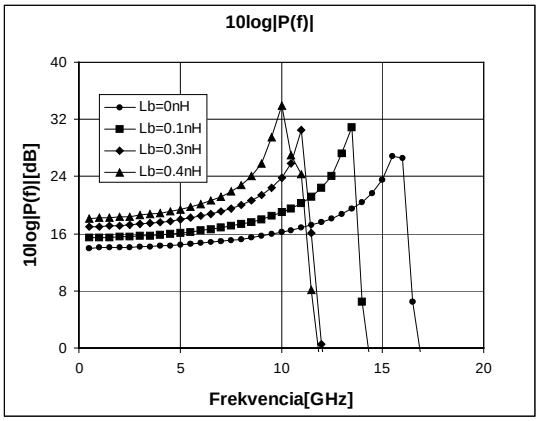

4.b)

Comparing it with the cut-off of the conventional connection (Eq. 5) it can be observed that the effect of L_B is only 2 times stronger than the effect of the interstage inductance. It is demonstrated in Fig. 4.b, where the power gain of a V-shape connected amplifier is shown, in which the element values are identical to that of the conventional DA of Fig. 3.a. The cut-off is significantly higher in Fig. 4.b.

Furthermore, very efficient reduction of the effect of the connection inductances can be achieved by substracking the connection inductances or a part of it from the interstage inductance.

Thesis 1.3. It gives closed formulas for the power-, voltage- and current gain, image impedances and propagation factor of a DA compriseing the input and output parasitic connection inductances of the active device. It is shown that presence of connection inductances the cut-off frequency decreases dramatically. The thesis proposes and analyzes the so-called V-shape connection to overcome this problem [S25, S26, S27].

THESIS GROUP 2.

The second thesis group deals with the so-called distributed element DA, in which the lumped interstage inductances are replaced by transmission lines (TLs). The schematic of a disrtibuted element, ideal amplifier is shown in Fig. 5.a. By means of the calculation method of thesis 1.1, one can derive the gains (power, voltage, current), propagation factor and image impedances of this kind of DAs. For example the power gain and the propagation factor is is given by Eq. 8 and Eq. 9, respectively. In the passband the propagation factor must be pure real in the loss free case, thus the inequality of Eq. 10 must be fullfilled. The left side equals to the right side at the starting frequency and at the end (cut-off) frequency of the pass band. However, the latter condition results a transcendental equation, which can not be solved in closed form. Thus, only approximate solution can be given for the cut-off frequency.

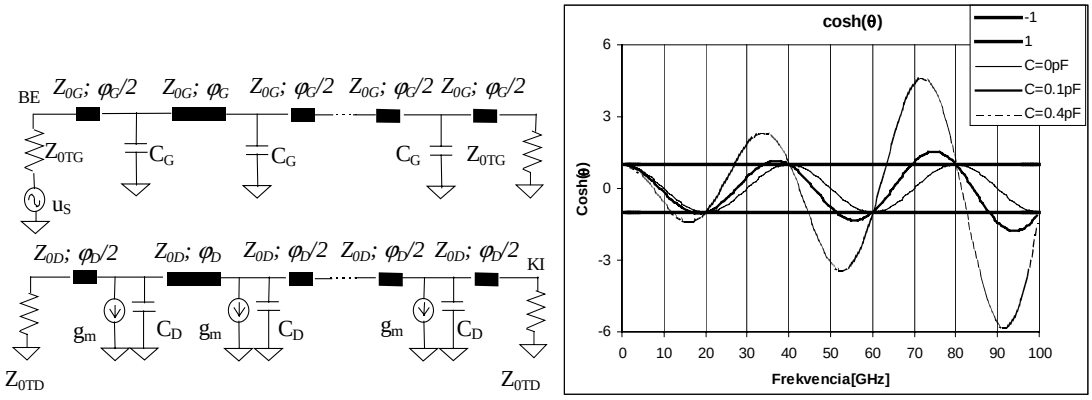

5.a) 5.b)

$$P = \frac{gm^2}{4} \frac{Z_{0TD} Z_{0TG}^{*} e^{-re(\theta_D - \theta_G)} e^{-2N\,re(\theta_D)}}{\left|1 + j\frac{Y_D Z_{0D}}{2} tan\left(\frac{\varphi_D}{2}\right)\right| \left|1 + j\frac{Y_G Z_{0G}}{2} tan\left(\frac{\varphi_G}{2}\right)\right|} \sum_{K=1}^{N} e^{K(\theta_D - \theta_G)} \sum_{K=1}^{N} e^{K(\theta_D - \theta_G)^{*}} \qquad 8$$

$$\theta = ar\cos h\left(\cos(\varphi) + j\frac{YZ_0}{2}\sin(\varphi)\right), \qquad 9$$

$$\left|\cos(\varphi) + j\frac{YZ_0}{2}\sin(\varphi)\right| \le 1, \text{ where } \varphi = \frac{\omega l}{v} \text{ and } Y = j\omega C \qquad 10$$

One possibility is to get the solution in graphical way, which is presented in Fig. 5.b. for several shunt capacitanve values (the physical length of the TL is constant: $l = 7.5mm$). As it can be seen if the capacitance is zero (the line of the DA become a single, loss free transmission line), the curve is between 1 and –1 at every frequency, i.e. the pass band is infinity. In the presence of any finite, positive capacitance the curve periodically exceeds the above-mentioned boundaries as the frequency increases, and between the tapered pass bands flared stop bands appear. It can be derived from Eq. 10., that at the begining of the pass bands the electrical lenght of the TLs must be integer multiplier of 2π ($\varphi = k2\pi$). From this condition and from the physical length of the TLs the starting frequencies can be calculated.

Thesis. 2.1. It gives closed formulas for the power, voltage, current gain, image impedances and propagation factor of a distributed element ideal DA. It is shown that the frequency characteristic, and the dependency on the shunt capacitance value of the image impedances and the propagation factor is very similar to that of the lumped element case. It demonstrates that in contradiction with the lumped element case infinite number of pass bands exist, which become narrower with increasing frequency. It gives approximate value for the cut-off frequency of the first pass band [S4, S19, S20].

The presence of parasitic connection inductances in distributed element DAs causes the same problems, which were observed in the case of lumped element amplifiers. In this case the schematic of the DA is very similar to that given by Fig. 3.a if the lumped inductances are replaced by TLs. For example the power gain is given by Eq. 11 for this case.

$$P^B = \frac{Z_{0TD} Z_{0TG}^{*} gm^2 \left|Y_G^B\right|^2 \left|Y_D^B\right|^2 e^{-re\left(\theta_G^B - \theta_D^B\right)} e^{-2N\, re\left(\theta_D^B\right)} \sum_{K=1}^{N} e^{K\left(\theta_D^B - \theta_G^B\right)} \sum_{K=1}^{N} e^{K\left(\theta_D^B - \theta_G^B\right)^*}}{4\left|Y_G\right|^2 \left|Y_D\right|^2 \left|1 + j\,\mathrm{tg}\left(\frac{\varphi_D}{2}\right)\frac{Y_D^B Z_{0D}}{2}\right| \left|1 + j\,\mathrm{tg}\left(\frac{\varphi_G}{2}\right)\frac{Y_G^B Z_{0G}}{2}\right|} \qquad 11$$

Thesis 2.2. It investigates the effect of the parasitic connection inductances in distributed element DAs. Closed formulas are derived for the power, voltage, current gain, image impedances and propagation factor. It is shown that similarly to the lumped element case the presence of the connection inductances strongly decrease the cut-off frequency and thus the gain-bandwidth product. The V-shape connection is also analyzed. The advantages are similar to the lumped element case [S4, S19, S20].

THESIS GROUP 3.

The third thesis group compares the properties of distributed element DAs to that of the lumped element DAs. The first part of the thesis investigates the dependency of the bandwidth on the physical lenght of the applied TLs. It is shown that by decreasing the physical length of the TLs the image impedances are also decreasing, and the cut-off frequency is increasing due to the decline of the distributed inductance. It is demonstrated in Fig. 6.a, where the image impedances vs. frequency is shown at different TL lenghts, at fixed shunt capacitance ($C= 0.4\ pF$) and characteristic impedance value (50 Ohm). The impedance-bandwidth product (IBP) of the image impedances can be compare very easely if the low frequency value of the image impedances is maintained on a constant value independently of the variation of the TL length. It can be achieved by the proper variation of the TL characteristic impedance (*Z0*) (f.e. at decreasing length the *Z0* must increase). The formula for *Z0* to keep the low frequency image impedances ($Z_{0T}(0)$) on a *k* constant value in case of *C* capacitance value and *l* TL lenght is given by Eq. 12.

$$Z0(Z_{0T}(0) = k, l, C) = \frac{1}{2l}\left(k^2 Cv + \sqrt{k^4 C^2 v^2 + 4l^2 k^2}\right) \qquad 12$$

As it can be observed in Fig. 6.b, where the TL characteristic impedance calculated by Eq. 12 is applied at different TL lengths ($C= 0.4\ pF$), in case of decreasing length the cut-off frequency and thus the IBP is increasing. The maximum is achieved at zero TL length, but according to Eq. 12, in this case the Z0 must be infinity, i.e. the cut-off frequency and thus the IBP is maximum if lumped inductances replace the TLs. It is also proved that the cut-off maximum equals to the cut-off of a lumped element DA line with the same impedance and shunt capacitance value. It can be also observed in Fig. 7.a. where the cut-off frequency vs. TL length is shown at different shunt capacitance values if the low frequency image impedances are kept at 50 Ohm. According to the previously presented power gain formulas, the GBP of a DA is proportional to the IBP of the image impedances if the phase mismatch (*q*) is not changing. Thus, it can be concluded that the lumped element DA has the highest GBP at a given active device.

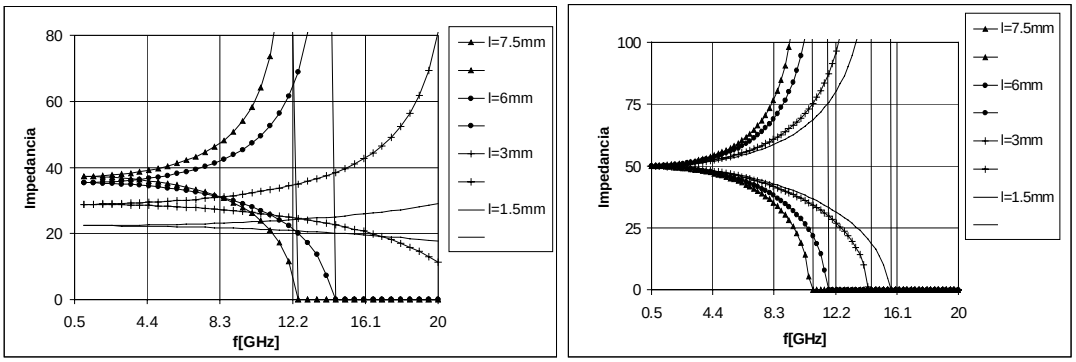

6.a) 6.b)

Thesis 3.1. It compares the gain-bandwidth product (GBP) of an ideal distributed element DA to that of an ideal lumped element DA through the comparison of the impedance-bandwidth product (IBP) of their image impedances, as the power gain is proportional to the IBP of the DA lines at a given *q* value. For the IBP comparison the low frequency value of the image impedances is maintained on a constant value by the proper adjustment of the TL characteristic impedance (calculation formula is also given), independently from the transmission line (TL) length. Thus the IBP is compared simply by the comparison of the cut-off frequencies. It is shown that by decreasing the TL length to zero the cut-off frequency increases monotonically and tends to that of the lumped element DA line. Hence, the thesis concludes that the lines of the lumped element DA has the highest IBP and thus the lumped element DA has the highest GBP with a given active device [S5, S11].

The same investigations are made in case of the presence of the parasitic connection inductances (L_B). Eq. 12 is also valid for the case of the conventionaly connected parasitic inductances as the image impedance value is independent from L_B. The cut-off frequency vs. TL length is given in Fig. 7.b at several L_B values at a fixed C (*0.4 pF*) and impedance value (*50 Ohm*). The curves tend to a maximum, to the lumped element cut-off

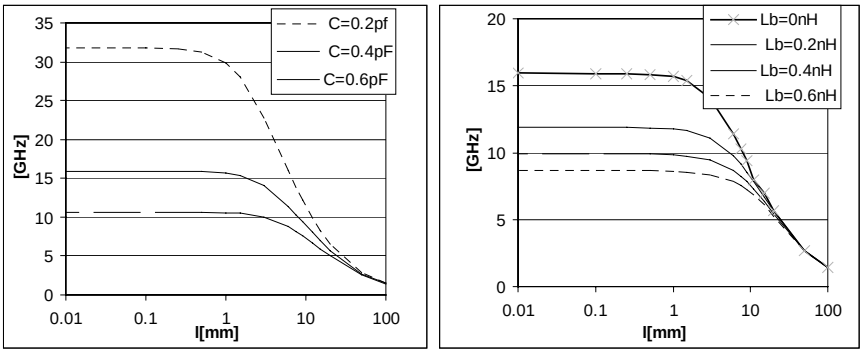

7.a) 7.b)

frequency at zero TL length. Thus, again the lumped element DA has the highest GBP.
In case of V-shape connection the formula to maintain the low frequency image impedances an a *k* konstant value is given by Eq. 13, as the impedance value is dependent on L_B. It is also proved that the lumped element V-shape connected DA has the highest GBP.

$$Z_0(k,\, l,\, C, L_B) = \frac{1}{2l}\left(k^2 C v - 2L_B v + \sqrt{k^4 C^2 v^2 + 4l^2 k^2 + 4L_B^2 v^2 - 4L_B v^2 k^2 C}\right) \qquad 13.$$

Thesis 3.2. It makes the investigations presented in Thesis 3.1 in case of the presence of the parasitic connection inductances (L_B). It shows that very similarly to the ideal case at a given shunt capacitance and L_B value the lumped element DA has the highest GBP value both in the conventionally connected and V-shape connected structure [S5, S7].

According to the previous results, during the design of a DA the phase mismatch (*q*) must be tuned to fullfill a gain charactersitic requirement, and on the other hand a refletion requirement must be satisfied up to a given operation frequency. In addition to this, if TLs are applied, the length of them must be as short as possible.

To fullfill all of these requirement a very flexible and independent variation of the image impedances and phase mismatch of the DA lines are necessary. In other words one should tune the image impedance value of a DA line independently from it's phase shift per section (propagation constant) even in case of fixed capacitance value. For this, the variation of the applied TL properties as well as the application of proper connection structure (V-shape or conventional) can be very efficient. Based on the results of the previous sections a systematic design procedure can create, which achieves flat (or any desired) gain characteristic up to a required frequency, in case of the presence of an unavoidable parasitic connection inductance. The design step are as follows:

1. Selecton of the active device. It should have low loss and negligible feedback capacitor value compared to the input and output capacitors. As the input capacitor is usually much higher than the output in a typical RF transistor, the input line restricts the bandwidth. The input capacitance value must be low enough to be able to fullfill the required reflection specification up to the required operation bandwidth. In this phase the proper choose of the connection structure is advantegous (usually V-shape connection is practical to widen the bandwidth). Beside that, one of the methods of Thesis 1.1 can also be used, which determinates the low frequency values of the image impedances of the input line.
2. Design of the input line. Knowing the necessary image impedance values, the input capacitance and the connection inductance, the characteristic impedance of the necessary TLs between the stages can be determined by the methods given in Thesis 3.2. The lenght of this TLs must be the technologically allowed minimum.
3. Determination of the necessary stage number to achieve the required gain. Knowing the input line impedance and assuming a drain line impedance of 50 Ohm the formulas available in the literature (described in detail in the first chapter of the Ph.D. thesis) can be used here.
4. Determination of the necessary phase mismatch between the input and output line of the DA. Here the structure of the drain line must be choosen as well, as the necessary *q* is depends on it. Due to the low output capacitance value usually the usage of conventional connection structure is practical. From the *q* and the input line bandwidth the necessary bandwidth for the output line can be determined.

Design of the drain line. Knowing the structure, output capacitance, connection inductance and the bandwidth the TLs for the output line can be designed. Fig. 8 shows a DA designed by the above method. It has the proposed hybrid structure. The applied transistor is unilateral (feedback capacitor is neglected). According to the specifications the power gain must be higher than 14 dB, and the reflections must be better than –20 dB up to 20 GHz, between 50 Ohm terminations. The input capacitance of the choosen transistor was 0.14pF. Together with the assumed minimum value of the connection inductance (0.3 nH) up to 22 GHz the reflection was predicted to be better than the required if the method of Thesis 1.2 is used. The simulated (NOT OPTIMIZED!!) gain and reflections are shown in Fig. 9.a and Fig. 9.b, respectively. They exactly follow the predicted properties without any optimization.

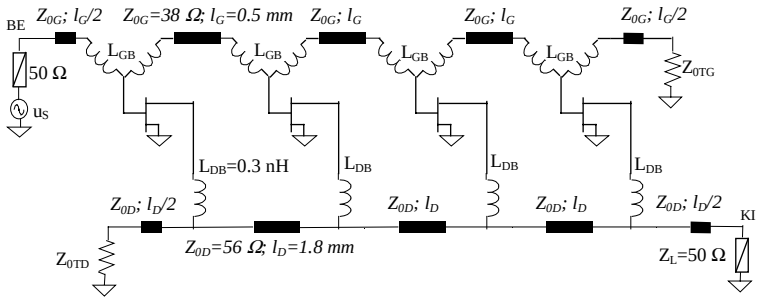

Fig. 8.

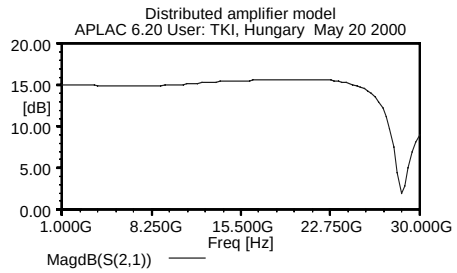

9.a)

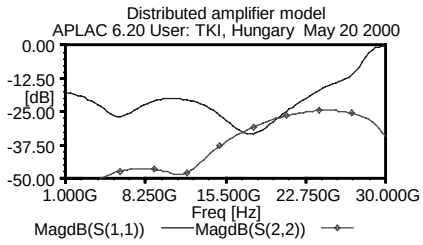

9.b)

The effect of finite feedback capacitor and loss is also investigated. It is shown, that in case of typical transistor loss values (f.e. Rg=5 Ohm, Rds=50 Ohm) the gain decrease near cut-off can be easely compensated by the slight decrease of the *q* value.

Thesis 3.3. It gives a design procedure, which by the proper choose of the DA structure and proper variation of the applied TLs tunes the phase mismatch between the DA lines, and by this way it synthetize a distributed element DA with flat gain and required input and output reflections. As the lengths of the applied TLs are as short as possible, according to the results of Thesis 3.1 and 3.2, the GBP is maximum with the given active device. It is shown that the effect of typical transistor losses can be easely compensated by the slight reduction of *q*. The effect of the feedback capacitor is also investigated. It is shown that if the feedback capacitor is less than the 40% of the output capacitor its effect can be easely compensated by computer optimization using the designed amplifier as a starting point [S2, S5, S7].

In the literature only one systematic design prosedure exists [21]. However, this graphical (thus, also approximate) method only valid for unilateral transistor model, for lumped element amplifiers and in case of phase synchone between the DA lines (*q=1*). The lumped element approach can not be used at very high frequencies. The creation of phase synchronisation can be very difficult in ideal, lumped element case as the strongly different input and output capacitance values of a typical RF transistor can only be equilazed by external elements, which can only be connected through unavoidable parasitics.
This method manipulates the losses of the transistors to get flat gain characteristic. The manipulation of transistor losses is simple only in monolithic circuits where the transistor geometries are changeable. However, the required higher loss value to compensate the pole at cut-off (as it is shown the effect of typical loss values is not significant), especially at the input, may degrades the noise properties of the amplifier, but at least makes the design of a proper active device much more difficult. The method proposed by Thesis 3.3 have restrictions only about the feedback capacitor value, thus gives much higher freedom during the design of the active device. The feedback capacitor value is very small in Hetero Junction Bipolar Transistors (HBT), thus the method is well applicable for DAs applying that devices. A commercially available HEMT type is also presented, which satisfy the feedback capacitor requirement.

Thesis 3.4. It shows several hybrid integrated DAs were realized in the framework of Copernicus research project of the European Union. Detailed analyzes of the realized amplifiers proves some results of the previous sections (effect of parasitic connection inductances, phase mismatch, calculation of operation frequency in Thesis 1.2 etc.) [S4, S6, S19, S22, S23, S27, S29, S31-35].

A realized two stage, hybrid integrated amplifier applying encapsulated HEMTs (HP-ATF35576) is shown in Fig. 10.a. This very early design was made by fully computer optimization methods without the knowledge of the design method of Thesis 3.3. Despite of that, several results of the previous chapters is proved on it (optimum structure, stage number, reflections and operational bandwidth etc.). The measured and simulated gain is given by Fig. 10.a. The noise figure is fairly low, its minimum value is 2.2 dB around 7 GHz.

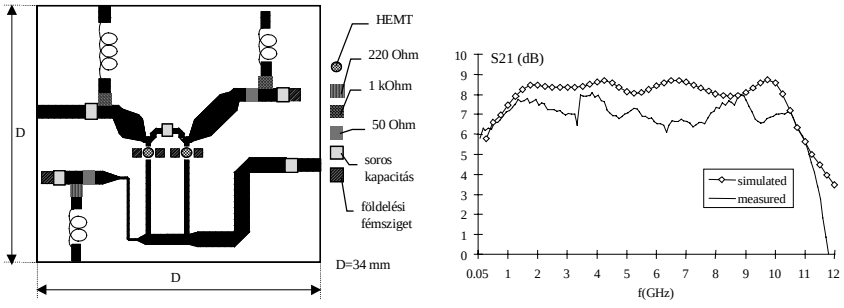

10.a) 10.b)

Based on this amplifier a photoreceiver was designed and built with the PD94CP-S12AR1300 type PIN photodiode of Opto-Speed. The photodiode was connected to the amplifier input through a tuned series bonding inductance. The picture of the photoreceiver and the measured responsibility is shown in Fig. 11.a and Fig. 11.b, respectively. The minimum of the measured input equivalent noise current density is approx. 10 pA/$\sqrt{Hz}$.

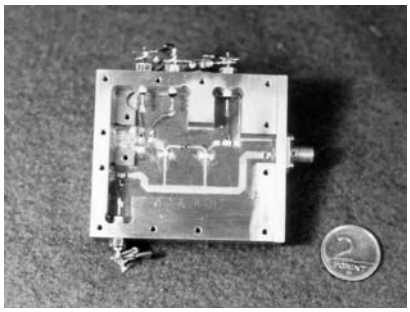

11.a)

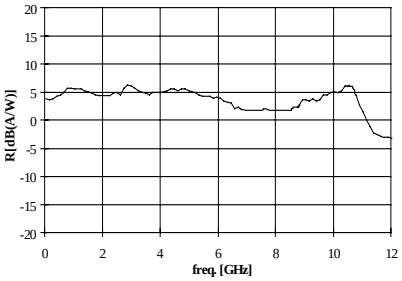

11.b)

The V-shape connection was realized on a two-stage hybrid integrated amplifier applying chip transistors. The picture of the amplifier and the structure is shown in Fig. 12.a and Fig. 12.b, respectively. Zoomed photo of the V-shape bonding and the measured S-parameters are shown in Fig. 13.a and 13.b, respectively.

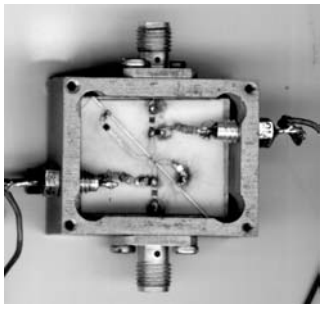

12.a)

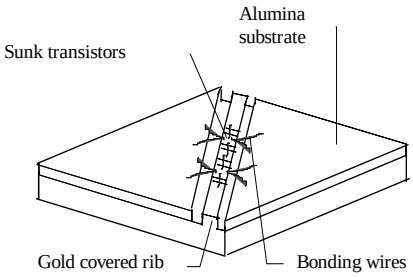

12.b)

13.a)

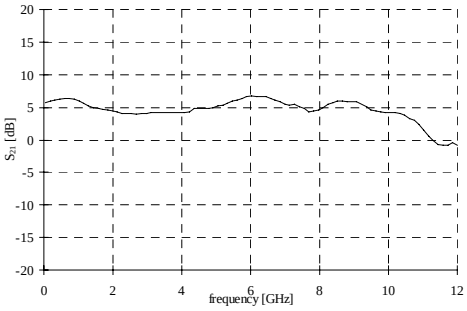

13.b)

THESIS GROUP 4.

The fourth thesis group deals with the analysis and design of harmonic oscillators, in which the aim is the proper adjustment of the harmonic content, especially the enhancement of the third harmonic level. This oscillator is well applicaple for frequency multiplication. This function is used in the base station of a proposed low cost optically feeded MMW picocell system, in which the MMW radio carrier is generated from an optically transmitted low frequency subcarrier as a reference. The block diagram of a system was realized by the team of Prof. Tibor Berceli in the framework of the FRANS research project of the European Union is shown in Fig. 14.

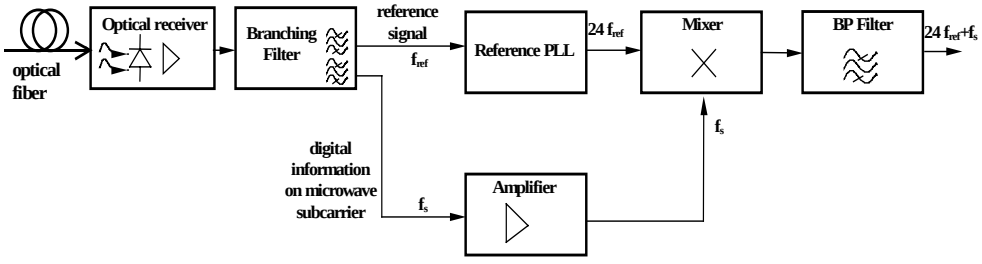

Fig. 14

The frequency multiplier PLL unit is shown in more detail in Fig. 15. As the member of the research team the author took part in the design and realization of several components. The main part of the

work was the design and realization of the harmonic VCO producing the MMW carrier as the third harmonic of the PLL loop frequency.

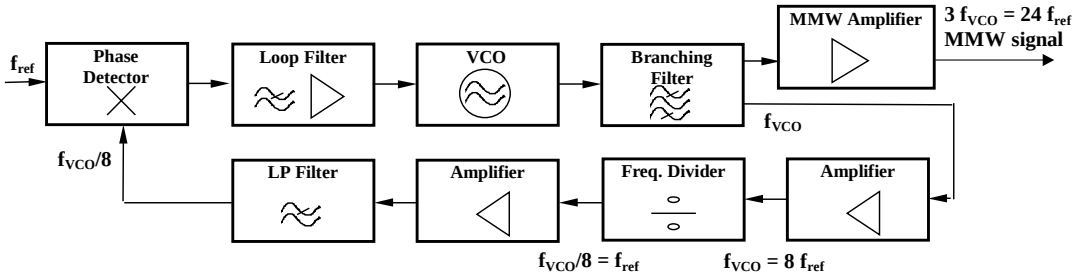

Fig. 15.

The analized oscillator model consists of a nonlinear, memory free voltage controlled current generator with zero phase shift and a linear feedback network. The current generator represents the transconductance of the active device, which is assumed to be much stronger nonlinear than any other parts in a typical transistor. Thus, the transistor parasitics are assumed to be linear and are involved to the linear feedback network together with the external elements and the phase shift of the transconductance, which is assumed again to be linear.
In further investigations MESFETs are used as an active device. The nonlineraty of the transconductance is measured at DC and approximated by a third order characteristic between the pinch-off and saturation voltage. Below the pinch-off voltage and above the saturation voltage the transconductance is assumed to be zero and constant, respectively. A typical MESFET transfer (Id-Ugs) characteristic is shown in Fig. 17.

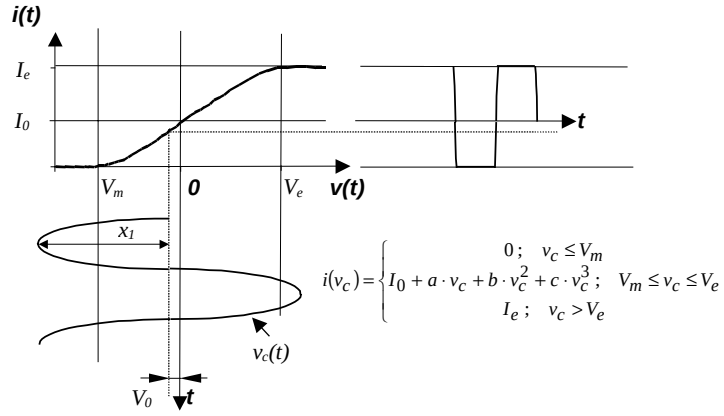

Fig. 16.

The magnitude of the oscillation i.e. the operation point of the oscillator can be manipulated by the linear transfer function of the feedback network, which is assumed to be nonzero only around the fundamental frequency. The output waveform and thus the harmonic content can be varied either by the oscillation magnitude or by the gate bias voltage. Hence the design of the oscillator is equivalent with the design of the transfer function of the feedback network.

Thesis 4.1. It applies the theoretical method presented by Bíró [60] to the description of MESFET harmonic oscillators. It is shown that the harmonic content can be optimized by the proper choice of the gate bias voltage and by the proper adjustment of the oscillation magnitude.

The output waveforms at different gate bias voltage and oscillation magnitudes can be classified into four operational types. Applying Fourier series, analythic expressions are derived for the fundamental, second and third harmonic magnitude at each operational type.
The resulting operational point must be stable, because only a stable operation point yields to a physically existing oscillation. By applying the theory of [60] general stability condition is derived for the two general feedback circuit type, which are given together with the stability conditions in Table 3. Using the reference directions given in the figure of Table 3, it is assumed that $D_{10}/X_{10}>0$, where D_{10} is the fundamental output and X_{10} is the input (fundamental) at the operation point. This condition means that the gain of the nonlinear part is positive. Parallel with this, the real part of the transfer function of the feedback circuit ($Hr(\omega_0)$) must be negative to have an operation point.

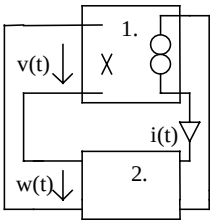

Feedback circuit type	Stability condition	Soft build-up condition
$H_r(\omega_0)<0;\quad H_i'(\omega_0)>0$	$\frac{D_{10}}{x_{10}}>\frac{dD_1}{dx_1};\quad x_1=x_{10}$	$\frac{D_{10}}{x_{10}}<\frac{dD_1}{dx_1};\quad x_1=0$
$H_r(\omega_0)<0;\quad H_i'(\omega_0)<0$	$\frac{D_{10}}{x_{10}}<\frac{dD_1}{dx_1};\quad x_1=x_{10}$	$\frac{D_{10}}{x_{10}}>\frac{dD_1}{dx_1};\quad x_1=0$

Table. 3.

The condition of soft build-up is also given. The oscillation will build-up softly if the zero magnitude as an operation point is instable.

Thesis 4.12. By modifying the method of Bíró [60] it gives general conditions for the investigation of stability of the operation point and soft build-up of the oscillation [S3 ,S9, S10, S12-S18, S21, S22, S24].

It is shown for the characteristic of Fig. 16, that in case of the first type feedback circuit the operation points are stable and the soft build-up condition is also satisfied at very wide range of gate bias voltages and magnitudes. In contradiction with this, in case of second feedback type, the soft build-up condition can not be satisfied, and the operation point is stable only in a narrow magnitude and gate voltage range. According to these results to achieve high third harmonic level strong, symmetrical overdrive of the active device is necessary.

The method is demonstrated by the realized harmonic VCO of the receiver of the FRANS research project. The fundamental and third harmonic ferquency was 8.44 GHz and 25.32 GHz, respectively. The picture of the VCO and the measured harmonic levels vs. varactor voltage is shown in Fig. 17.a and Fig. 17.b, respectively.

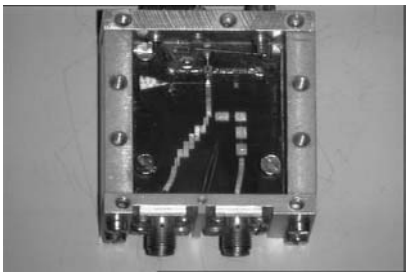

17.a)

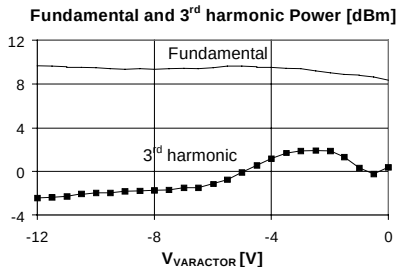

17.b)

Thesis 4.2. It gives a more accurate prediction of the output power levels by taking into account three secondary effect at the high current, saturation region of the transfer (transconductance) characteristic of the active device. They ar e as follows: the reduction of the drain current due to the current suck of the open gate-source diode at high input magnitudes, effect of series input losses and reduction of the feedback circuit transfer characteristic in case of opened gate-source diode.

The first phenomenon can be observed at high positive peaks of the input signal when a part of the electrons travel to the positive gate instead of the drain. Hence, the drain current is decreases. The phenomena can be measured and taken into account by modifying the transfer characteristic. It is demonstrated in Fig. 18.a, where a measured characteristic is shown. The deviation of the calculated fundamental and third harmonic level from the measured value is less than 2.6dB if the modified characteristic of Fig. 18.a is used.

In case of the second phenomenon, due to the gate current which flowing through the series gate (Rg) and series intrinsic (Ri) resistors and due to the gate and drain current which flowing through the series source (Rs) resistors, only a small part of the input signal drives the transconductance. It can be taken into account in the transfer characteristic by the reduction of the gate voltage, where the gate current is not zero. This modified characteristic is presented in Fig. 18.b.

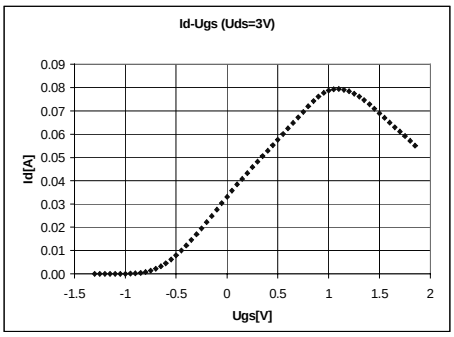

18.a)

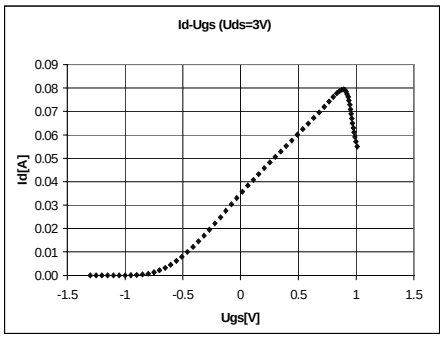

18.b)

In the previous two cases the transfer characteristic is divided into five subsections and approximated polinoms are derived to each section. Three of them: a third order, a linear and a zero section describes the saturation region. The remaining two is the same as it was in the case of Thesis 4.1 (zero below pinch-off, and third order between pinch-off and saturation). Due to the increasing number of the sections the output waveforms can be described by 8 different operation type.

In the third phenomenon the opened gate-source diode reduce the transfer characteristic of the feerdback circuit at the positive peaks of the input signal. Due to this the feedback circuit transfer characteristic become nonlinear. By neglecting the nonlinerarity of the imaginary part the used simple method is still applicable. Knowing the nonlinearity of the real part (see Fig. 19.a) the transfer function for the fundamental can be derived (denoted by $F_1(H_r(\omega_0))$ in Fig. 19.b. The reciproc of this must be equal to the fundamental gain of the transconductance at the operation point. The whole procedure is shown in Fig. 19.b. After determination of the fundamental, the stability can be investigated by the method of Thesis 4.12 and the third harmonic level can be calculated. The deviation from the measured fundamental and third harmonic level was less than 2 dB in this case.

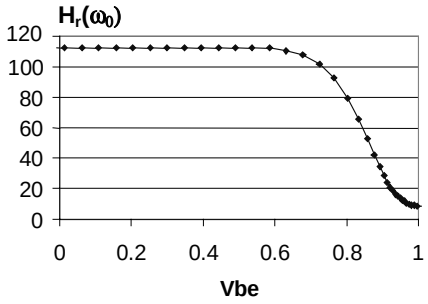

19.a)

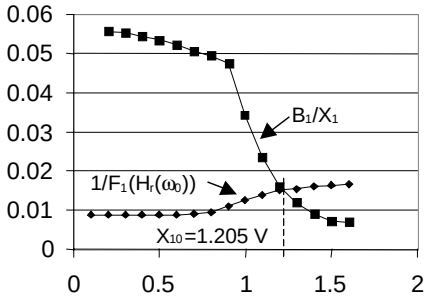

19.b)

Publications of the author in the field of the Ph.D. thesis.

[S1] Berceli, Frigyes, Hilt, Járó, Lénárt, Mihály, Marozsák, Szekeres, Szûcs, **Zólomy** : "Optikai Hálózatok Méréstechnikája", *Budapesti Mûszaki Egyetem, Mérnöktovábbképzõ Intézet ,tanfolyami segédlet*, április 1997. (in hungarian)

Journal paper

[S2] **A.Zólomy** : " Synthesis Method for Distributed Amplifiers" *Journal of Telecommunications and Information Technology*, Vol. 1, pp. 20-23, 2003, L

[S3] T.Berceli, G.Járó, T.Marozsák, S.Mihály, E.Udvary, Z.Varga, **A.Zólomy** : "An Optical Carrier Generation Approach for Cellular Millimeter-Wave Radio Systems" Fiber and Integrated Optics, Vol. 19, No.2, pp. 119-136, 2000, The Netherlands, L

[S4] **A. Zólomy**, T. Berceli, , G. Járó, A. Hilt, T. Marozsák : "Low Noise Optical Receiver With Multioctave Bandwidth", *Invited Paper for Optical and Quantum Electronics*, Vol. 30 pp. 969-983, Dec, 1998, USA, L

[S5] **A. Zólomy**, "Extrém sávszélességű elosztott erősítők tervezése", *Híradástechnika*, 2003. Augusztus, L (in hungarian)

[S6] G.Járó, A.Hilt, **A.Zólomy**, T.Berceli : "Noise Properties of Optical Receivers Using Distributed Amplification", *Journal on Communications, Vol. XLVIII*, pp. 31-34, August, 1997, Hungary, L

Conference paper

[**S7**] A. Zólomy : "Synthesis Method for Distributed Amplifiers", *MIKON'2002, International Conference on Microwaves & Radar*, proceedings CD, Gdansk, Poland, May 20-22, 2002, L, R. (fiatal kutatók verseny 2. Helyezés)

[S8] **A. Zólomy** : "Design Method for Distributed Amplifiers with Parasitic Input and Output Lead Inductances of the Active Devices", Proc. of Optical/Wireless Workshop in the framework of the European MOIKIT project, pp 15-18, Budapest, Hungary, March 15, 2001.

[S9] T. Berceli, S.Kudszus, M.Schlechtweg, **A. Zólomy**, G. Járó, T. Marozsák : "Optical Millimeter Wave Generation Utilizing a Subhamonic Reference", Proc. of IEEE MTT-S ISM Digest, Vol. 3, pp. 1749-1752, Boston, Massachusetts, 2000, R

[S10] Berceli, G. Járó, T. Marozsák, S. Mihály, E. Udvary, Z. Varga, **A. Zólomy**: "Optical Millimeter Wave Generation for Cellular Mobile Systems", *Invited Paper, MIKON'2000, International Conference on Microwaves & Radar*, Vol. 3, pp. 110-119, Wroclaw, Poland, May 22-24, 2000, L, R

[S11] **A. Zólomy**: "Gain-Bandwidth Performance Comparison of Lumped and Distributed Element Distributed Amplifiers", *MIKON'2000, International Conference on Microwaves & Radar*, Vol. 1, pp. 101-104, Wroclaw, Poland, May 22-24, 2000, L, R

[S12] Berceli, G. Járó, T. Marozsák, S. Mihály, E. Udvary, Z. Varga, **A. Zólomy** : "A Novel Optical Cellular Millimeter Wave Radio System",, ", Proc. of the *29th* European Microwave Conference *(EuMC)*, Vol. pp. 230-233, München, Germany, October 5-7, 1999

[S13] Berceli, G. Járó, T. Marozsák,S. Mihály, E. Udvary, Z. Varga, **A. Zólomy** : "A New Optical Signal Distribution Method for Phased Array Antennas at Millimetre Waves", *Proceedings of the 5th International Conference on Radar System, Sesion2.2*, France, May 17-21, 1999.

[S14] **A. Zólomy**, V. Bíró : "A New Approach for Millimeter Waves Harmonic Oscillators", *Proceedings of the 10th MICROCOLL*, pp.235-239, Budapest, Hungary, March, 1999, L

[S15] Berceli, G. Járó, T. Marozsák, A. Hilt,S. Mihály, E. Udvary, **A. Zólomy**, Z. Varga : "Optical Generation of Millimeter Waves for Mobile Radio Systems", *Proceedings of the 10th MICROCOLL*, pp.375-378, Budapest, Hungary, March, 1999, L

[S16] A.Hilt, T.Berceli, A.Vilcot, G.Maury, **A.Zólomy** : "Radio Frequency Interference in Radio-Over-Fiber Distributed Networks", *Proceedings of the 10th MICROCOLL*, pp.149-152, Budapest, Hungary, March, 1999, L

[S17] **A. Zólomy**, V. Bíró, T. Berceli, G. Járó, A. Hilt: "Design of Nonlinear Oscillations for Millimeter Wave Signal Generation in Optical Systems*", Proc. of the European Microwave Conference*, EuMC'98, Vol.I, pp. 74-79, Amsterdam, October,1998.

[S18] T.Marozsák, T.Berceli, G.Járó, **A.Zólomy**, A.Hilt, S.Mihály, E.Udvary, Z.Varga : "A New Optical Distribution Approach for Millimeter wave radio" *IEEE-MWP'98 International Topical Meeting on Microwave Photonics, Technical Digest*, pp. 63-66, Princetown, USA, October 1998., L, R

[S19] T Berceli, **A. Zólomy**, G. Járó, A. Hilt, T. Marozsák :"Broadband Low Noise Optical Receiver Utilizing Distributed Amplification", *Invited Papers, MIKON'98, International Conference on Microwaves & Radar*, Vol. 4, pp. 135-146, Krakow, Poland, May 20-22, 1998, L, R

[S20] **Zólomy**, A. Hilt, G. Járó, T. Berceli :"The Effect Of Parasitic Inductances In Distributed Amplifiers*" Conference Proceedings, MIKON'98, International Conference on Microwaves & Radar*, Poland, Vol. 3., pp 463-467, Krakow, May 20-22, 1998, L, R

[S21] A. Hilt, **A. Zólomy**, T. Berceli, G. Járó, E. Udvary : "Millimeter Wave Synthesizer Locked to an Optically Transmitted Reference Using Harmonic Mixing", *IEEE-MWP'97 International Topical Meeting on Microwave Photonics, Technical Digest*, Duisburg, Germany, pp. 91-94, 3-5 September 1997, L, R

[S22] G.Járó, T.Berceli, A.Hilt, **A.Zólomy** : "New optomixer surpassing photodetection at microwaves", IEEE-*MWP'97 International Topical Meeting on Microwave Photonics, Technical Digest*, pp.143-146, Duisburg, Germany, September, 1997, L, R, H2

[S23] **A.Zólomy**, T.Berceli, A.Hilt, G.Járó, C.S.Aitchison, A.Baranyi, J.Ladvánszky, J.Y.Liang : "Eight Octave Bandwidth Optical Receiver Using Distributed Amplification", *IEEE-MWP'97 International Topical Meeting on Microwave Photonics, Technical Digest*, pp.147-150, Duisburg, Germany, September, 1997, L, R,

[S24] E. Udvary, **A. Zólomy**, A. Hilt, G. Járó, S. Mihály, T. Berceli : "A Millimeter Wave PLL oscillator for Optical Receivers", *Proc of First Electronic Circuits and Systems Conference, ECS'97*, pp. 205-208, Bratislava, Slovakia, 1997.

[S25] G.Járó, T.Berceli, A.Hilt, **A.Zólomy** : "Gain and Noise Optimization of an Optical Receiver Utilizing a Distributed Amplifier", *proceedings of ECCTD'97*, pp. 1356-1359, Budapest, Hungary, August 1997.

[S26] **A.Zólomy**, A.Hilt, A.Baranyi, G.Járó : "Microwave Distributed Amplifier In Hybrid Integrated Technology", *proceedings of ECCTD'97*, pp. 1374-1377, Budapest, Hungary, August 1997.

[S27] **A.Zólomy**, A.Hilt, T.Marozsák, G.Járó : "New Topology for Distributed Amplifiers in Hybrid Integrated Technology", *COMITE'97 Conference Proceedings*, pp.37-40, Pardubice, Czech Republic, 1997.

[S28] A.Hilt, G.Járó, **A.Zólomy**, B. Cabon, T.Berceli, T.Marozsák : "Microwave Characterization of High Speed pin Photodiodes", *COMITE'97 Conference Proceedings*, pp.21-24, Pardubice, Czech Republic, 1997, H1

[S29] **A.Zólomy**, G.Járó, A.Hilt, A.Baranyi, J.Ladvánszky : "Wideband Distributed Amplifier Using Encapsulated HEMTs", *Advanced NATO Research Workshop*, Sozopol, Bulgaria, September 1996, Horst Groll and Ivan Nedkov ed. : "Microwave Physics and Techniques", NATO ASI Series, 3-Vol.33, pp. 315-320, Kluwer Academic Publishers, Dordrecht, Boston, London, ISBN 0-7923-4582-7, H1

[S30] G.Járó, J.Ladvánszky, **A.Zólomy**, C.S.Aitchison, A.Baranyi, T.Berceli, J.Y.Liang : "Noise Minimization in Photodiode Driven Distributed Amplifiers*", proceedings of the 25th European Microwave Conference*, pp. 179-184, Bologna, Italy, September, 1995.

Reports and presentations

Research reports

S31] C.S.Aitchison, T.Berceli, A.Hilt, G.Járó, J.Y.Liang, T.Marozsák, **A.Zólomy** : "Improvement in Microwave to Optical Communication System Interfaces*" Final Report of the Copernicus EC Project, No.C6665, Brunel University, UK, Research Institute for Telecommunications and Technical University of Budapest, Hungary*, January 1997.

[S32] T.Berceli, A.Hilt, G.Járó, T.Marozsák, **A.Zólomy** : "Frans (Fiber to Radio ATM Network Services) Extension, Electrical Method", Progress Report, February 1997, TUB, Hungary

[S33] T.Berceli, A.Hilt, G.Járó, T.Marozsák, **A.Zólomy**, E.Udvary : "Frans Extension, Electrical Method" , Progress Report, September 1997, TUB, Hungary

[S34] T.Berceli, A.Hilt, G.Járó, T.Marozsák, S.Mihály, **A.Zólomy**, E. Udvary: "Frans Extension, Electrical Method", Progress Report, December 1998, TUB, Hungary[S35] T.Berceli, A.Hilt, G.Járó, T.Marozsák, S.Mihály, **A.Zólomy**, E. Udvary: "Frans Extension, Electrical Method", Progress Report, May 1999, TUB, Hungary

Oral presentation

[S34] **A.Zólomy**, T.Berceli, A.Baranyi, A.Hilt : "Design of Distributed Amplifiers for Optical Receivers", Seminar On Optical & Microwave Subsystems, TUB at the Department of Microwave Telecommunications, Hungary, September, 1997

Reference list

First author :

Referenced paper :

[S29] A.Zólomy, G.Járó, A.Hilt, A.Baranyi, J.Ladvánszky : "Wideband Distributed Amplifier Using Encapsulated HEMTs", *Advanced NATO Research Workshop*, Sozopol, Bulgaria, September 1996, *and Horst Groll and Ivan Nedkov ed.: "Microwave Physics and Techniques", NATO ASI Series, 3-Vol.33, pp.315-320, Kluwer Academic Publishers, ISBN 0-7923-4582-7*, Dordrecht, Boston, London.

Reference :

(r1) ref [2] in B.Y.Banyamin, J.Y.Liang and C.S.Aitchison : "A New High Gain-Broadband Amplifier Using Cascaded Single Stage Distributed Amplifiers", *Proc. of the Asia Pacific Microwave Conference, pp.753-756,* Yokohama, Japan, 8-11 December 1998.
text : (page 753, ref. 2) "This distributed amplifier has been thoroughly investigated and realised successfully in hybrid and monolitic technology in number of publications [1-4]"

Co-author:

Referenced paper:

[S21] A.Hilt, **A.Zólomy**, T.Berceli, G.Járó, E.Udvary : "Millimeter Wave Synthesizer Locked to an Optically Transmitted Reference Using Harmonic Mixing", *Technical Digest of the IEEE Topical Meeting on Microwave Photonics, MWP'97, pp.91-94,* Duisburg, Germany, 3-5 September 1997.

Reference :

(r2) ref. [16] in Ichiro Seto, Hiroki Shoki, Shigeru Ohshima : "Optical Subcarrier Multiplexing Transmission for Base Station With Adaptive Array Antenna", *IEEE Transactions on Microwave Theory and Techniques, Vol. 49, No. 10, Pp.2036-2041*, October 2001.
Text: (page 2039, ref. 16) "…In that case, a higher frequency of the clock reference is desirable and other PLL structures are also of interest [16]…."

Referenced paper:

[S28] A.Hilt, G.Járó, **A.Zólomy**, B.Cabon, T.Berceli, T.Marozsák : "Microwave Characterization of High Speed pin Photodiodes", *Proc. of the, 9th Conference on Microwave Techniques, COMITE'97, pp.21-24,* Pardubice, Czech Republic, October 1997.

Reference :

(h3) ref. [9] in F.Giannini, E.Limiti, G.Orengo, G.Saggio : "Broadband Low Noise HEMT-Based Monolithic Transimpedance Amplifier", *Proc. of the 10th Microwave Colloquium, MICROCOLL'99, pp.171-173,* Budapest, Hungary, March 1999.
Text: (page 172, ref. 9) "…Cpd is the photodetector parasitic capacitance [9]."

Referenced paper:

[S22] G.Járó, T.Berceli, A.Hilt, **A.Zólomy** : "New optomixer surpassing photodetection at microwaves", *Technical Digest of the IEEE MTT Topical Meeting on Microwave Photonics, MWP'97, pp.143-146,* Duisburg, Germany, 3-5 September 1997.

Reference ::

(h4) ref. [39] in Bogdan A.Galwas : "Photonic Technology for Microwave Engineering", *invited paper, Proc. of the International Conference on Microwaves and Radar, MIKON'98, Vol.4, pp.117-134,* Kraków, Poland, 20-22 May 1998.
Text: (page 124, ref. 39) : "Then optical-microwave conversion takes place within the diode [36,39,43,55]"

(h5) ref. [5] in S.K.Banerjee, U.Goebel, P.Nüchter : "An X-Band Balanced Optical Hybrid Mixer for □-Wave Optical Interconnect in Active Phased Array Radar and Communication Systems", *Technical Digest of the IEEE International Topical Meeting on Microwave Photonics, MWP'2000, paper WE2.13, pp.198-202, ISBN 0-7803-6455-4,* Oxford, UK, 11-13 September 2000.
Text (page 202, ref. 5) :"Reference [5]"

Referenced paper :

[S18] T.Marozsák, T.Berceli, G.Járó, **A.Zólomy**, A.Hilt, S.Mihály, E.Udvary, Z.Varga : "A New Optical Distribution Approach for Millimeter Wave Radio", *Proc. of the IEEE MTT Topical Meeting on Microwave Photonics, MWP'98, pp.63-66,* Princeton, New Jersey, USA, 12-14 October, 1998.

Reference :

(h6) ref. [9] in Masahiro Kiyokawa, J.Claude Bélisle, Pierre Tardif : "Millimeter-wave Fiber Radio Using Subharmonic Local-Oscillator Distribution", *Proc. of the IEEE MTT Topical Meeting on Microwave Photonics, MWP'2001*, 2001.
Text: (page 124, ref. 39) : "….Many approaches have been proposed to generate and distribute MMW signals to and from the remote sites [7]- [13]…..The ILPLL approach was experimentally pursued in [9]."

Referenced paper :

[S10] T.Berceli, G.Járó, T.Marozsák, S.Mihály, E.Udvary, Z.Varga, **A.Zólomy** : "Optical Millimeter Wave Generation for Cellular Mobile Systems", *paper invited for Proc. of the XIIIth International Conference on Microwaves, Radar and Wireless Communications, MIKON'2000, Vol.3., pp.110-119,* Wroclaw, Poland, 22-24 May 2000.

Reference :

(h7) ref. [31] in Hamed Al-Raweshidi, Shozo Komaki editors: "Radio over Fiber technologies for Mobile Communications Networks", István Frigyes : "Basic Microwave properties of Optical Links : Insertion Loss, Noise Figure, and Modulation Transfer", *pp.1-63, Artech House*, Boston, London, UK, 2002.